Flocking in Teams of Nonholonomic Agents

Herbert G. Tanner[1], Ali Jadbabaie[2], and George J. Pappas[3]

[1] Mechanical Engineering Department, MSC01 1150, University of New Mexico, Albuquerque NM 87131 tanner@unm.edu
[2] Electrical and Systems Engineering Department, University of Pennsylvania, 200 South 33rd Street, Philadelphia PA 19104 jadbabai@seas.upenn.edu
[3] Electrical and Systems Engineering Department, University of Pennsylvania, 200 South 33rd Street, Philadelphia PA 19104 pappasg@ee.upenn.edu

Summary. The motion of a group of nonholonomic mobile agents is synchronized using local control laws. This synchronization strategy is inspired by the early flocking model proposed by Reynolds [23] and following work [30, 9]. The control laws presented ensure that all agent headings and speeds converge asymptotically to the same value and collisions between the agents are avoided. The stability of this type of motion is closely related to the connectivity properties of the underlying interconnection graph. Proof techniques are based on LaSalle's invariant principle and algebraic graph theory and the results are verified in numerical simulations.

1 Introduction

Technological advances in computation and communication have provided efficient and inexpensive means to compute and share information. This breakthrough facilitates the development of new multi-agent systems, that promise increased performance, efficiency and robustness. Networked, large scale multi-agent systems are currently been deployed in several fields, from automotive and aerospace to wireless networks, and operate successfully at a fraction of the cost of alternative centralized desings.

Nature is abundant in marvelous examples of coordinated behavior. Across the scale, from biochemical cellular networks, up to ant colonies, schools of fish, flocks of birds and herds of land animals, one can find systems that exhibit astonishingly efficient and robust coordination schemes [1, 18, 32, 8, 5]. At the same time, several researchers in the area of statistical physics and complexity theory have addressed flocking and schooling behavior in the context of non-equilibrium phenomena in many-degree-of-freedom dynamical systems and self organization in systems of self-propelled particles [30, 29, 28, 16, 14, 25, 11]. Similar problems have become a major thrust in systems and control theory, in the context of cooperative control, distributed control of multiple vehicles and formation control; see for example [13, 2, 19, 22, 4, 15, 6, 26, 9, 17,

3, 10, 31, 20]. The main objective in multi-vehicle control designs presented in the above papers is to develop a decentralized strategy, so as to achieve a common goal, such as a tight formation with fixed pair-wise inter vehicle distances.

Synchronization phenomena in nature, engineering and social sciences have always fascinated the research community [21]. One of the first popular applications of models for multi-agent coordination, was the field of computer animation. In 1986 Craig Reynolds [23] made a computer model of coordinated animal motion such as bird flocks and fish schools. He named the generic simulated flocking creatures "boids". The basic flocking model consists of three simple steering behaviors which describe how an individual boid maneuvers based on the positions and velocities its nearby flockmates:separation, alignment, and cohesion:

- **Separation:** steer to avoid crowding local flockmates.
- **Alignment:** steer towards the average heading of local flockmates.
- **Cohesion:** steer to move toward the average position of local flockmates.

This work inspired significant efforts in this direction that culminated in the birth of a new field in computer graphics called artificial life [27].

In 1995, a similar model was proposed by Vicsek *et al.* [30]. Under an alignment rule, a spontaneous development of coherent collective motion is observed, resulting in the headings of all agents to converge to a common value. The first rigorous proof of convergence of Vicsek's model (for the noise-free case) was given in [9].

In this paper we introduce a set of local control laws that essentially realize Reynold's rules. In our interpretation of Reynold's approach, we consider dynamic models of nonholonomic mobile agents steered by local control inputs that enable them to avoid collisions with each other and move coherently in a common direction. Each mobile agent is described by nonholonomic differential equations of the form:

$$\dot{x}_i = v_i \cos\theta_i \tag{1a}$$

$$\dot{y}_i = v_i \sin\theta_i \tag{1b}$$

$$\dot{\theta}_i = \omega_i \tag{1c}$$

$$\dot{v}_i = a_i, \tag{1d}$$

for i ranging from 1 to N, which is the total number of agents in the group. In the above, $r_i = (x_i, y_i)^T$ is the position vector of vehicle i, θ_i its orientation (Figure 1), v_i its translational speed, and a_i, ω_i its control inputs. The relative positions between the vehicles are denoted $r_{ij} \triangleq r_i - r_j$.

The control inputs are assumed to have two components. The first is responsible for synchronizing the headings and the speeds of the mobile agents, while the second steers them so that they avoid collisions. Collision avoidance is realized through local artificial potential fields. [12, 24]. For the system of mobile agents we show that all agent headings converge to the same value,

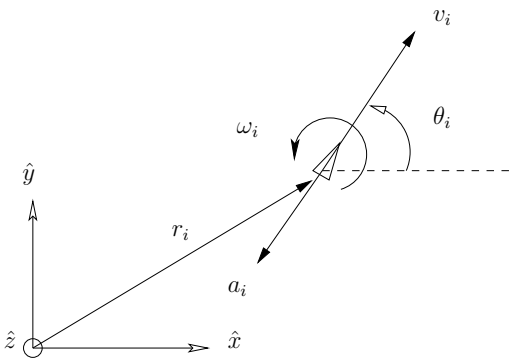

Fig. 1. Agent i and its control inputs.

and pairwise relative speeds are stabilized. As a result, the group maintains its shape and moves uniformly in a common direction.

Our analysis is based on Lyapunov stability and algebraic graph theory. Central to this analysis is the connectivity of the graph that represents control interactions between the agents. If the interconnection graph is connected at all times, then headings and speeds of all agents converge to the same value. In fact, the higher the algebraic connectivity of the graph, the faster the convergence. This result provides a direct link between the connectivity of the interconnection network and the stability and robustness properties of the group.

2 Algebraic Graph Theory

The stability results derived in this work rely heavily on the algebraic properties of a certain graph that represents control interconnections between agents in the group. This section provides a brief introduction to basic graph-related terminology and notation in order for the rest of the discussion to proceed smoothly. For a detailed treatment of algebraic properties of graphs, see [7]. A reader familiar with graph theory may safely proceed directly to Section 3.

An (undirected) *graph* $\mathcal{G}$ consists of a *vertex set*, $\mathcal{V}$, and an *edge set* $\mathcal{E}$, where an edge is an unordered pair of distinct vertices in $\mathcal{G}$. If $x, y \in \mathcal{V}$, and $(x, y) \in \mathcal{E}$, then x and y are said to be *adjacent*, or neighbors and we denote this by writing $x \sim y$. A graph is called *complete* if any two vertices are neighbors. A *path* of length r from vertex x to vertex y is a sequence of $r+1$ distinct vertices starting with x and ending with y such that consecutive vertices are adjacent. If there is a path between any two vertices of a graph $\mathcal{G}$, then $\mathcal{G}$ is said to be *connected*.

An *orientation* of a graph $\mathcal{G}$ is the assignment of a direction to each edge, so that the edge (i, j) is now an arc from vertex i to vertex j. We denote by $\mathcal{G}^\sigma$

the graph $\mathcal{G}$ with orientation σ. The *incidence matrix* $B(\mathcal{G}^\sigma)$ of an oriented graph $\mathcal{G}^\sigma$ is the matrix whose rows and columns are indexed by the vertices and edges of $\mathcal{G}$ respectively, such that the i, j entry of $B(\mathcal{G}^\sigma)$ is equal to 1 if edge j is incoming to vertex i, -1 if edge j is outcoming from vertex i, and 0 otherwise. The symmetric matrix defined as:

$$L(\mathcal{G}) = B(\mathcal{G}^\sigma)B(\mathcal{G}^\sigma)^T$$

is called the *Laplacian* of $\mathcal{G}$ and is independent of the choice of orientation σ. It is known that the Laplacian captures many interesting properties of the graph. Among those, is the fact that L is always symmetric and positive semidefinite, and the algebraic multiplicity of its zero eigenvalue is equal to the number of connected components in the graph. For a connected graph, the n-dimensional eigenvector associated with the single zero eigenvalue is the vector of ones, $\mathbf{1}_n$. The second smallest eigenvalue, λ_2 is positive and is known as the algebraic connectivity of the graph, because it is directly related to how the nodes are interconnected.

3 Coordination Strategy

In a group of N mobile agents with dynamics given by (1), each agent i is assumed to have access to state information from a subset of the agent group called its neighbor set. This neighboring set, denoted $\mathcal{N}_i \subseteq \{1, \ldots, N\} \setminus \{i\}$, can include agents the state of which agent i can obtain through sensing or through direct communication. The ability to exchange state information thus define a neighboring relation between two agents. The topology of these relations is represented by means of an acyclic graph:

Definition 1 (Neighboring graph). *The neighboring graph, $\mathcal{G} = \{\mathcal{V}, \mathcal{E}\}$, is an undirected graph consisting of:*

- *a set of vertices (nodes), $\mathcal{V} = \{n_1, \ldots, n_N\}$, indexed by the agents in the group, and*
- *a set of edges, $\mathcal{E} = \{(n_i, n_j) \in \mathcal{V} \times \mathcal{V} \mid n_i \sim n_j\}$, containing unordered pairs of nodes that represent neighboring relations.*

In the sequel we will assume that the neighboring graph is connected and time invariant. This implies that the neighboring sets remain the same for all time.

For a pair of neighboring agents, $(i, j) \in \mathcal{E}$ we define an artificial potential function V_{ij} that depends on the distance between these two agents. An example of such function, given here for illustration purposes, is the following:

$$V_{ij}(\|r_{ij}\|) = \frac{1}{\|r_{ij}\|^2} + \log \|r_{ij}\|^2 .$$

The potential of an agent i, is now defined as the sum of all artificial potentials associated with every one of its neighbors:

$$V_i \triangleq \sum_{j \in \mathcal{N}_i} V_{ij}(\|r_{ij}\|).$$

The control law for agent i is now defined as follows:

$$a_i = -k \sum_{j \in \mathcal{N}_i} (v_i - v_j) - \langle \nabla_{r_i} V_i, (\cos\theta_i, \sin\theta_i) \rangle \, |\textstyle\sum_{j \in \mathcal{N}_i} (v_i - v_j)| \tag{2a}$$

$$\omega_i = -k \sum_{j \in \mathcal{N}_i} (\theta_i - \theta_j) - \langle \nabla_{r_i} V_i, (-\sin\theta_i, \cos\theta_i) \rangle \, |\textstyle\sum_{j \in \mathcal{N}_i} (\theta_i - \theta_j)|, \tag{2b}$$

where k is a positive control gain and $\langle \cdot \rangle$ denotes the dot vector product. For the closed loop system we can now prove that the agent headings and speeds are going to converge to the same value.

Proposition 1 (Flocking of Nonholonomic Agents). *Consider the system of N mobile agents with dynamics* (1)*. Then, for a sufficiently large control gain k, the agent headings and speeds converge to the same value.*

Proof. Consider the positive semi-definite function

$$V = \frac{1}{2} \boldsymbol{\theta}^{\mathrm{T}} \mathsf{L}_c \boldsymbol{\theta} + \frac{1}{2} \boldsymbol{v}^{\mathrm{T}} \mathsf{L}_c \boldsymbol{v}, \tag{3}$$

where $\boldsymbol{\theta}$ and $\boldsymbol{v}$ are the stack vectors of the agent headings and speeds, respectively, and L_c is the Laplacian of the complete graph with N vertices. Denoting L the Laplacian of the neighboring graph and taking the derivative of V with respect to time, we obtain:

$$\dot{V} = -\boldsymbol{\theta}^{\mathrm{T}} \mathsf{L}_c \left(k \mathsf{L} \boldsymbol{\theta} + |\mathsf{L}\boldsymbol{\theta}| \begin{bmatrix} (\nabla_{r_1} V_i)_\perp & & 0 \\ & \ddots & \\ 0 & & (\nabla_{r_N} V_N)_\perp \end{bmatrix} \right) - \boldsymbol{v}^{\mathrm{T}} \mathsf{L}_c \left(k \mathsf{L} \boldsymbol{v} + \begin{bmatrix} (\nabla_{r_1} V_i)_\parallel & & 0 \\ & \ddots & \\ 0 & & (\nabla_{r_N} V_N)_\parallel \end{bmatrix} \right),$$

where $(\nabla_{r_i} V_i)_\parallel$ and $(\nabla_{r_i} V_i)_\perp$ are the components of $\nabla_{r_i} V_i$ when expressed in a body-fixed coordinate frame, aligned with the velocity of agent i. Using the fact that $\mathsf{L}_c = N\mathsf{I} - \mathsf{J}$, where I is the $N \times N$ identity matrix and J is the $N \times N$ matrix of ones, the above simplifies to:

$$\dot{V} = -kN(\boldsymbol{\theta}^{\mathrm{T}} \mathsf{L} \boldsymbol{\theta} + \boldsymbol{v}^{\mathrm{T}} \mathsf{L} \boldsymbol{v}) - |\mathsf{L}\boldsymbol{\theta}| \boldsymbol{\theta}^{\mathrm{T}} \mathsf{L}_c \begin{bmatrix} (\nabla_{r_1} V_i)_\perp & & 0 \\ & \ddots & \\ 0 & & (\nabla_{r_N} V_N)_\perp \end{bmatrix} - |\mathsf{L}\boldsymbol{v}| \boldsymbol{v}^{\mathrm{T}} \mathsf{L}_c \begin{bmatrix} (\nabla_{r_1} V_i)_\parallel & & 0 \\ & \ddots & \\ 0 & & (\nabla_{r_N} V_N)_\parallel \end{bmatrix}. \tag{4}$$

Components of $\boldsymbol{v}$ and $\boldsymbol{\theta}$ along the direction of the vector of ones, $\mathbf{1}$, preserve the value of V. To see this, decompose $\boldsymbol{v}$ and $\boldsymbol{\theta}$ as $\boldsymbol{\theta} = \boldsymbol{\theta}^{1} \oplus \boldsymbol{\theta}^{1^{\perp}}$ and $\boldsymbol{v} = \boldsymbol{v}^{1} \oplus \boldsymbol{v}^{1^{\perp}}$, respectively, Superscripts 1 and $1^{\perp}$ denote the components along the direction of the vector of ones and its orthogonal. Then, (4) becomes

$$\begin{aligned}
\dot{V} =& -k(\boldsymbol{\theta}^{1^{\perp}})^{\mathrm{T}} \left(N\mathsf{L}\boldsymbol{\theta}^{1^{\perp}} + \mathsf{L}_c \left\| \mathsf{L}\boldsymbol{\theta}^{1^{\perp}} \right\| \begin{bmatrix} (\nabla_{r_1} V_i)_{\perp} & & 0 \\ & \ddots & \\ 0 & & (\nabla_{r_N} V_N)_{\perp} \end{bmatrix} \right) \\
& -k(\boldsymbol{v}^{1^{\perp}})^{\mathrm{T}} \left(kN\mathsf{L}\boldsymbol{v}^{1^{\perp}} + \mathsf{L}_c \left\| \mathsf{L}\boldsymbol{v}^{1^{\perp}} \right\| \begin{bmatrix} (\nabla_{r_1} V_i)_{\parallel} & & 0 \\ & \ddots & \\ 0 & & (\nabla_{r_N} V_N)_{\parallel} \end{bmatrix} \right) \\
\leq & -kN\lambda_2 \|\boldsymbol{\theta}^{1^{\perp}}\|^2 + \|\boldsymbol{\theta}^{1^{\perp}}\| \, \|\mathsf{L}_c\| \, \|\mathrm{diag}\{(\nabla_{r_i} V_i)_{\perp}\}\| \sqrt{N} \|\mathsf{L}\boldsymbol{\theta}^{1^{\perp}}\| \\
& -kN\lambda_2 \|\boldsymbol{v}^{1^{\perp}}\|^2 + \|\boldsymbol{v}^{1^{\perp}}\| \, \|\mathsf{L}_c\| \, \left\|\mathrm{diag}\{(\nabla_{r_i} V_i)_{\parallel}\}\right\| \sqrt{N} \|\mathsf{L}\boldsymbol{v}^{1^{\perp}}\| \\
\leq & -N(k\lambda_2 - N\sqrt{N} f_{max}) \|\boldsymbol{\theta}^{1^{\perp}}\|^2 - N(k\lambda_2 - N\sqrt{N} f_{max}) \|\boldsymbol{v}^{1^{\perp}}\|^2, \quad (5)
\end{aligned}$$

where f_{max} is the magnitude of the maximum potential force. Choosing

$$k \geq \frac{N\sqrt{N} f_{max}}{\lambda_2},$$

ensures that V will be decreasing. Any level set of V is invariant and from (3) all speed and heading differences have to remain bounded. Given that $\boldsymbol{v}^{1^{\perp}} = \boldsymbol{\theta}^{1^{\perp}} = 0$ is an equilibrium configuration for (1), application of LaSalle's invariant principle shows that this configuration is asymptotically stable:

$$\dot{V} = 0 \Rightarrow \|\boldsymbol{\theta}^{1^{\perp}}\| = \|\boldsymbol{v}^{1^{\perp}}\| = 0,$$

implying that $\boldsymbol{\theta}$ and $\boldsymbol{v}$ are parallel to $\mathbf{1}$:

$$\theta_1 = \cdots = \theta_N = \bar{\theta}, \qquad\qquad v_1 = \cdots = v_N = \bar{v},$$

and substituting in (2a) and (2b) we see that

$$\omega_1 = \cdots = \omega_N = 0, \qquad\qquad a_1 = \cdots = a_N = 0.$$

Thus, (1) is now

$$\dot{x}_i = \bar{v} \cos\bar{\theta}, \qquad\qquad \dot{y}_i = \bar{v} \sin\bar{\theta}.$$

□

4 Simulations

Consider a group of 10 mobile agents. First assume that the neighboring graph is complete, that is, every agent is interconnected to every other agent. The

initial (x, y) coordinates of each agent are selected randomly in the interval $[-5, 5]$ m, its speed is taken in random within the interval $[-1, 1]$ m/s and headings belong $[-\pi, \pi]$. Control gain k is set to 1.

We depict the evolution of a set of $N - 1 = 9$ heading differences that span the relative headings space in Figure 2. Figure 2 shows that the heading differences have converged exponentially to zero after approximately 10 simulation seconds, resulting in all agents moving in the same direction.

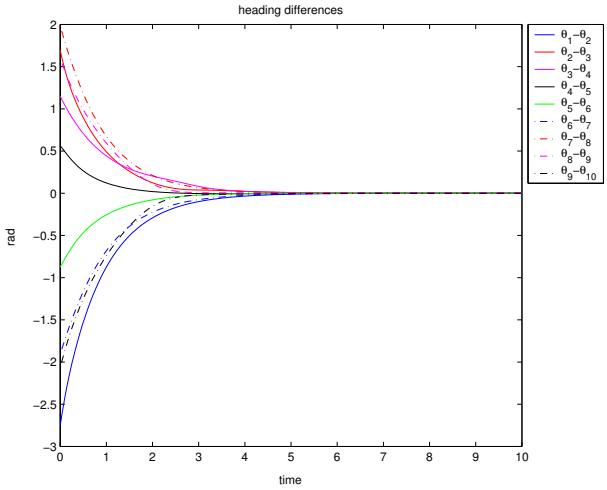

Fig. 2. Convergence of headings when the interconnection graph is complete.

Figure 3 shows the convergence of speeds. In Figure 3 the speeds of the 10 agents converge exponentially to the same value, which is approximately 0.5m/s.

Figures 4-5 refer to the case where the neighboring graph is not complete, i.e. it does not have all possible edges, but it is nevertheless connected. The evolution of same set of heading differences as in the previous case is now depicted in Figure 4. The Figure shows that the headings still converge to the same value, however the rate of convergence is smaller and it takes almost 15 simulation seconds to reach steady state. This is due to the fact that in this case, the second eigenvalue of the graph Laplacian, λ_2 is smaller. Recall from (5) that λ_2 is related to the convergence rate of the Lyapunov-like function.

The evolution of the agent speeds is given in Figure 5. Speeds converge exponentially to a value close to 0.7m/s. Note once again that due to the reduced value of λ_2, the agent speeds take longer to reach their steady state compared to the case of the complete interconnection graph.

In Figure 6 one can see the paths followed by the agents during another simulation instance, starting again from random initial conditions. The agents

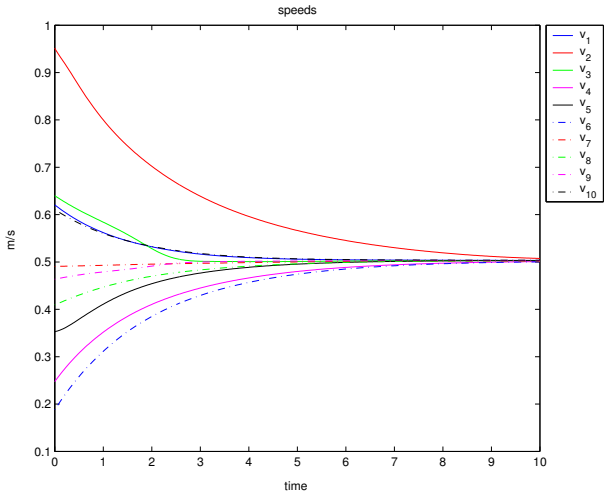

Fig. 3. Convergence of speeds when the interconnection graph is complete.

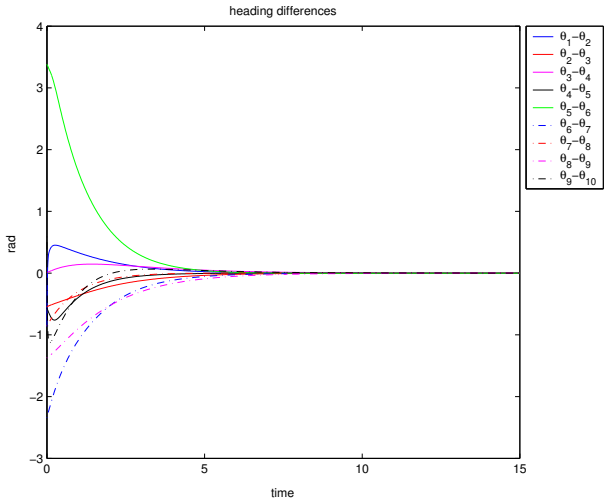

Fig. 4. Convergence of speeds when the interconnection graph is incomplete but connected.

in this Figure are shown as dots whereas their paths are given by dashed lines. Line segments connecting different agents denote constant neighboring relationships and the arrows attached to each dot correspond to their velocities.

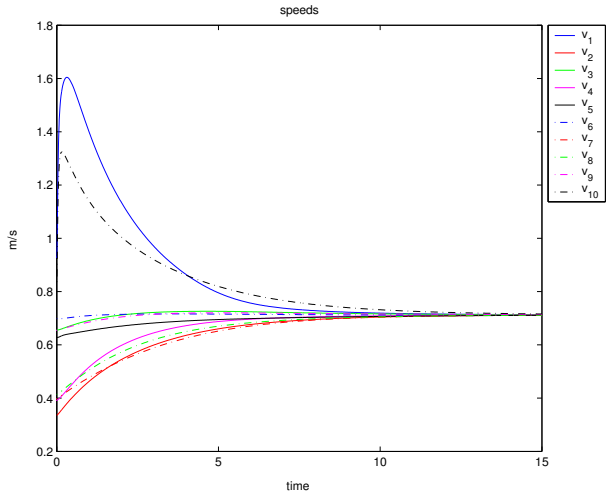

Fig. 5. Convergence of speeds when the interconnection graph is connected but not complete.

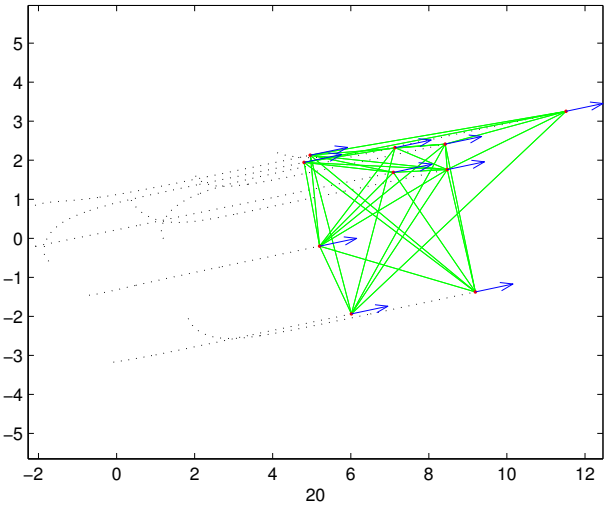

Fig. 6. Paths and steady state velocities of a group of ten agents.

5 Conclusions

In this work we show how a group of nonholonomic mobile agents can synchronize their headings and speeds using local control laws. These control laws are constructed as a combination of a synchronization term that drives each agent speed and heading to the average over its set of neighbors and a sector

bounded artificial potential term that steers the agent towards a direction that minimizes its potential and keeps it from colliding with its neighbors. Stability analysis makes use of Lyapunov theory and known results from algebraic graph theory. This is where the topology of interconnection is reflected on the stability and robustness properties of the group. The dependence of convergence speed to the degree of connectivity in the interconnection graph becomes evident in simulation examples.

References

1. C. M. Breder. Equations descriptive of fish schools and other animal aggergations. *Ecology*, 35:361–370, 1954.
2. Jorge Cortes, Sonia Martinez, Timur Karatas, and Francesco Bullo. Coverage control for mobile sensing networks. *IEEE Transactions on Robotics and Automation*, 2002. (submitted).
3. J. P. Desai, J. P. Ostrowski, and V. Kumar. Modeling and control of formations of nonholonomic mobile robots. *IEEE Transactions on Robotics and Automation*, 17(6):905–908, 2001.
4. J. Alexander Fax and Richard M. Murray. Graph Laplacians and stabilization of vehicle formations. *15th IFAC Congress, Barcelona, Spain*, 2002.
5. G. Flierl, D. Grunbaum, S. Levin, and D. Olson. From individuals to aggregations: the interplay between behavior and physics. *Journal of Theoretical Biology*, 196:397–454, 1999.
6. V. Gazi and K. M. Passino. Stability analysis of swarms. *IEEE Transactions on Automatic Control*, 48(4):692–696, April 2003.
7. C. Godsil and G. Royle. *Algebraic Graph Theory*. Springer Graduate Texts in Mathematics # 207, New York, 2001.
8. D. Grunbaum and A. Okubo. Modeling social animal aggregations. *Frontiers in Theoretical Biology*, 100 of Lecture Notes in Biomathematics:296–325, 1994.
9. A. Jadbabaie, J. Lin, and A. S. Morse. Coordination of groups of mobile autonomous agents using nearest neighbor rules. *IEEE Transactions on Automatic Control*, 48(6):988–1001, July 2002.
10. E.W. Justh and P.S. Krishnaprasad. A simple control law for UAV formation flying. Technical Report 2002-38, Institute for Systems Research, 2002.
11. M. Kardar, G. Parisi, and Y.-C. Zhang. Dynamic scaling of growing interfaces. *Physical Review Letters*, 56:889–892, 1986.
12. Oussama Khatib. Real-time obstacle avoidance for manipulators and mobile robots. *The International Journal of Robotics Research*, 5(1):396–404, Spring 1986.
13. N. Leonard and E. Friorelli. Virtual leaders, artificial potentials and coordinated control of groups. *IEEE Conference on Decision and Control*, 2001.
14. H. Levine and W. J. Rappel. Self organization in systems of self-propelled particles. *Physical Review E*, 63:208–211, 2001.
15. Y. Liu, K. M. Passino, and M. M. Polycarpou. Stability analysis of m-dimensional asynchronous swarms with a fixed communication topology. *IEEE Transactions on Automatic Control*, 48(1):76–95, February 2003.
16. A. S. Mikhailov and D. Zannette. Noise induced breakdown of collective coherent motion in swarms. *Physical Review E*, 60:4571–4575, 1999.

17. P. Ögren, M. Egerstedt, and X. Hu. A control Lyapunov function approach to multi-agent coordination. *IEEE Transactions on Robotics and Automation*, 18, October 2002.
18. A Okubo. Dynamical aspects of animal grouping: swarms, schools, flocks, and herds. *Advances in Biophysics*, 22:1–94, 1986.
19. R. Olfati and R. M. Murray. Distributed structural stabilization and tracking for formations of dynamic multi-agents. In *IEEE Conference on Decision and Control*, Las Vegas, NV, 2002.
20. Aniruddha Pand, Pete Seiler, T. John Koo, and Karl Hedrick. Mesh stability of unmanned aerial vehicle clusters. In *Proceedings of the American Control Conference*, pages 62–68, Arlington, VA, June 2001.
21. Arkady Pikovsky, Michael Rosenblum, and Jurgen Kurths. *Synchronization: A Universal Concept in Nonlinear Science*. Cambridge Nonlinear Science. Cambridge University Press, 2002.
22. John H. Reif and Hongyang Wang. Social potential fields: A distributed behavioral control for autonomous robots. *Robotics and Autonomous Systems*, 27:171–194, 1999.
23. C. Reynolds. Flocks, birds, and schools: a distributed behavioral model. *Computer Graphics*, 21:25–34, 1987.
24. E. Rimon and D. Koditschek. Exact robot navigation using artificial potential functions. *IEEE Transactions on Robotics and Automation*, 8(5):501–518, October 1992.
25. N. Shimoyama, K. Sugawa, T. Mizuguchi, Y. Hayakawa, and M. Sano. Collective motion in a system of motile elements. *Physical Review Letters*, 76:3879–3873, 1996.
26. P. Tabuada, G. J. Pappas, and P. Lima. Feasible formations of multi-agent systems. In *Proceedings of the American Control Conference*, Arlington, VA, 2001.
27. D. Terzopoulos. Artificial life for computer graphics. *Communications of the ACM*, 42(8):32–42, 1999.
28. J. Toner and Y. Tu. Long range order in a two dimensional xy model: How birds fly together. *Physical Review Letters*, 75:4326–4329, 1995.
29. J. Toner and Y. Tu. Flocks, herds, and schools: A quantitative theory of flocking. *Physical Review E.*, 58:4828–4858, 1998.
30. T. Vicsek, A. Czirok, E. Ben Jacob, I. Cohen, and O. Schochet. Novel type of phase transitions in a system of self-driven particles. *Physical Review Letters*, 75:1226–1229, 1995.
31. R. Vidal, O. Shakernia, and S. Sastry. Distributed formation control with omnidirectional vision based motion segmentation and visual servoing. *Robotics and Autonomous Magazine*, 2003. (to appear).
32. K. Warburton and J. Lazarus. Tendency-distance models of social cohesion in animal groups. *Journal of Theoretical Biology*, 150:473–488, 1991.